Environmental Research 167 (2018) 515–523

Contents lists available at ScienceDirect

Environmental Research

journal homepage: www.elsevier.com/locate/envres

A simple model for estimating changes in rainfall erosivity caused by variations in rainfall patterns

Gabriel P. Lobo[a], Carlos A. Bonilla[a,b,*]

[a] Departamento de Ingeniería Hidráulica y Ambiental, Pontificia Universidad Católica de Chile, Av. Vicuña Mackenna 4860, Macul, Santiago, Chile
[b] Centro de Desarrollo Urbano Sustentable CONICYT/FONDAP/15110020, El Comendador 1916, Providencia, Santiago 7520245, Chile

ARTICLE INFO

Keywords:
CLIGEN
Daily rainfall
Erosivity
Global circulation models
Soil loss
RUSLE

ABSTRACT

A major challenge when coupling soil loss models with precipitation forecasts from Global Circulation Models (GCMs) is that their time resolutions do not generally agree. Precipitation forecasts from GCM must be scaled down; however, the distribution of the rainfall intensity, which can affect soil loss as much as precipitation amounts, is usually not considered in this process. Therefore, the objective of this study was to develop a statistical equation for computing event-based rainfall erosivity under changing precipitation patterns using the least amount of information possible. For this purpose, an empirical equation for predicting event-based rainfall erosivity was developed using the product of the total precipitation P and the maximum 0.5-h rainfall intensity, $I_{0.5}$. This equation was calibrated using measured precipitation data from 28 sites in Central Chile and then tested with simulated data with different rainfall patterns from the CLIGEN (CLImate GENerator) weather generator. More than 53,000 rainfall events were analyzed, where the equation consistently provided R^2 values of 0.99 for every dataset used, revealing its robustness when used in potential climate change scenarios in the study site. However, because computing $I_{0.5}$ requires estimating precipitation at a high time resolution, the relationship was recalibrated and tested using 1 through 24-h maximum rainfall intensities. Using these intensities, the equation provided erosivity estimates with R^2 ranging from 0.78 to 0.99, where better results were obtained as the resolution of the data increased. This study provides the methodology for building and testing the proposed equation and discusses its advantages and limitations.

1. Introduction

Soil erosion caused by rainfall is likely to change as a consequence of climate change for a number of reasons, including altered plant biomass production, precipitation patterns, microbial activity and evapotranspiration rates, among others (Boardman and Favis-Mortlock, 1993; Nearing, 2001; Asselman et al., 2003). Global circulation models (GCMs) are currently the most widely used tools for quantifying the impacts of climate change, as they provide long-term forecasts for precipitation and temperatures, among other variables (Samadi et al., 2010). GCMs may be coupled with soil loss models to estimate soil loss under different climate change scenarios; however, doing so is challenging because these models operate at different time scales (Morrison et al., 2002). While GCMs provide monthly forecasts, soil loss models usually require daily or instant precipitation data (Samadi et al., 2010), thus, GCM forecasts are usually downscaled when integrating climate change scenarios into soil loss models (Xu, 1999).

Several strategies have been used to downscale GCM data to make them compatible with soil loss models. One strategy is to use stochastic climate generators, such as the Climate Generator (CLIGEN) (Nicks et al., 1995), to downscale the GCM forecasts into individual rainfall events (von Storch, 1999; Nearing et al., 2004; Samadi et al., 2010; Hoomehr et al., 2016). By altering parameters that affect precipitation amounts, occurrence and rainfall intensity, these weather generators can be adjusted to provide monthly precipitation amounts that agree with GCM forecasts (Yu, 2005; Burton et al., 2009). However, choosing the right parameters to adjust is challenging, as there are infinite possible combinations of rainfall intensity, duration and occurrence that can add up to a monthly climate change scenario. All of these variables affect the erosive power of rainfall (Lobo and Bonilla, 2015) and hence the soil loss process. Thus, choosing which parameters to alter is an important aspect to consider when using climate generators to downscale monthly GCM forecasts, which adds a great degree of uncertainty when using this method.

* Corresponding author at: Departamento de Ingeniería Hidráulica y Ambiental, Pontificia Universidad Católica de Chile, Av. Vicuña Mackenna 4860, Macul, Santiago, Chile.
E-mail address: cbonilla@ing.puc.cl (C.A. Bonilla).

https://doi.org/10.1016/j.envres.2018.08.009
Received 5 January 2018; Received in revised form 3 August 2018; Accepted 3 August 2018
Available online 06 August 2018
0013-9351/

Table 1
Location and rainfall characteristics of the 28 climate stations in the study area.

Station	Latitude	Longitude	Elevation (m.a.s.l.)	Measurement period	Years of hourly rainfall records	Years of missing rainfall data	Total number of events	Annual rainfall depth (mm)	Average rainfall intensity (mm h^{-1})	I_1 (mm h^{-1})	$I_{0.5}$
Pedernal	32°05' S	70°48' W	1100	1972–1992	21	0	226	40	0.3	2.5	2.8
Sobrante	32°14' S	70°47' W	810	1972–1992	21	0	271	46	0.3	2.0	2.3
Quillota	32°54' S	71°13' W	130	2004–2013	10	0	141	35	0.3	2.6	3.0
Lliu Lliu	33°06' S	71°13' W	260	1979–1992	14	0	324	139	0.5	3.5	4.0
Pirque	33°40' S	70°35' W	670	1979–1980	2	0	67	183	0.5	2.3	2.6
Melipilla	33°41' S	71°12' W	170	1975–1992	18	0	485	136	0.4	2.7	3.1
Rengo	34°25' S	70°52' W	310	1970–1992	23	0	771	169	0.5	2.5	2.9
Popeta	34°26' S	70°47' W	400	1970–1974	6	1	158	152	0.5	3.1	3.5
Central Las Nieves	34°30' S	70°43' W	700	1971–1992	22	0	716	287	0.5	3.1	3.5
Potrero Grande	35°11' S	71°06' W	460	1972–1992	21	0	758	316	0.7	3.7	4.1
Fundo Peral	35°24' S	71°47' W	110	1974–1986	13	0	532	353	0.5	2.7	3.1
Colorado	35°38' S	71°16' W	420	1969–1992	24	0	1065	532	0.8	4.0	4.5
Melozal	35°46' S	71°47' W	110	1971–1992	22	0	825	227	0.5	2.6	3.0
Ancoa	35°54' S	71°17' W	430	1971–1992	22	0	881	532	0.9	4.0	4.5
Bullileo	36°17' S	71°25' W	600	1971–1992	22	0	1298	1236	1.1	5.0	5.5
Chillan Viejo	36°38' S	72°06' W	125	1984–1992	9	0	634	511	0.7	3.0	3.6
Coihueco	36°39' S	71°48' W	300	1984–1992	8	1	616	709	0.9	3.1	3.5
Caracol	36°39' S	71°23' W	620	1987–1992	6	0	326	972	1.0	4.2	4.6
Diguillin	36°52' S	71°39' W	670	1965–1992	28	0	1413	770	0.9	3.9	4.3
Quilaco	37°41' S	71°60' W	225	1965–1992	28	0	1752	786	0.8	3.6	4.2
Cerro el Padre	37°47' S	71°52' W	400	1976–1992	17	0	1226	1067	0.9	3.8	4.3
El Vergel	37°49' S	72°39' W	75	1976–1981	5	1	268	307	0.5	2.4	2.8
Contulmo	38°01' S	73°14' W	25	1987–1992	4	2	157	236	0.4	3.2	3.8
Traiguén	38°15' S	72°40' W	170	1988–1992	5	0	373	506	0.5	2.4	2.8
Manzanar	38°28' S	71°42' W	790	1972–1988	17	0	1135	831	0.8	3.3	3.8
Pueblo Nuevo	38°44' S	72°34' W	100	1989–1992	4	0	396	444	0.5	2.2	2.6
Freire Sendos	38°58' S	72°37' W	100	1985–1987	3	0	166	316	0.5	2.8	3.3
Pucón	39°17' S	71°57' W	230	2005–2013	9	0	823	1042	0.7	2.9	3.3

Another widely used alternative for integrating GCM forecasts to soil loss models is to use statistical methods that relate GCM data with rainfall erosivity, a commonly used parameter when estimating soil loss (Nearing et al., 2005; Klik and Eitzinger, 2010; Mondal et al., 2016). Rainfall erosivity provides a measure of the kinetic energy of the raindrops and hence the capacity of rainfall to detach soil particles, and it is used in the Revised Universal Soil Loss Equation (RUSLE) (Renard et al., 1991) and the 2nd version of RUSLE (RUSLE2) (Foster, 2008). To compute rainfall erosivity based on GCM data, Nearing (2001) used monthly precipitation forecasts and statistical relationships between monthly rainfall and annual rainfall erosivity to compute soil loss using the RUSLE. This allowed obtaining long-term annual erosion estimates for different climate change scenarios. However, the main limitation of this method is that it does not provide a tool for simulating individual soil loss events, which is paramount when designing effective soil and water conservation practices (Erol and Randhir, 2013). Moreover, there is no guarantee that the statistical relationships between monthly rainfall and annual erosivity will hold if rainfall patterns change due to climate change.

Panagos et al. (2017) developed another statistical method, in which they computed daily rainfall erosivity based on correlations between recorded rainfall patterns and climate data using a Gaussian Process Regression model. By using a long-term, high-resolution climate dataset from Europe, and correlating precipitation patterns to other climate variables and erosivity, they obtained accurate erosivity estimates for different climate change scenarios. However, methods such as this one, although effective, are only viable in locations where detailed climate information is available, limiting its use.

Currently, there are no simple empirical equations for estimating daily rainfall erosivity, which would allow identifying the key climate variables needed to model soil loss. Identifying such variables is important for reducing the uncertainty associated with current GCM downscaling methods, as it would reduce the number of variables needed to model erosivity and soil loss. Predicting rainfall erosivity requires knowledge of several variables, including storm duration, mean and maximum intensity and rainfall amounts, among others, all of which are currently predicted with a great degree of uncertainty. Therefore, the objective of this study was to develop a statistical equation for computing event-based rainfall erosivity under changing precipitation patterns using the least amount of information possible. By correlating erosivity with several commonly used storm parameters from measured rainfall data of 28 sites in Central Chile, a statistical relationship was developed. This relationship was then tested for simulated rainfall events using CLIGEN with modified rainfall intensities, storm durations, and precipitation amounts and patterns, all of which represented different hypothetical climate change scenarios. The results of this study are meant to help identify the minimum number of variables required for forecasting soil loss using GCMs, while discussing the advantages and limitations of commonly used GCM precipitation forecast downscaling methods.

2. Materials and methods

2.1. Study area

The data used in this study were obtained from the 28 meteorological stations shown in Table 1, which are located in Central Chile and distributed between latitudes 32°04'S and 39°47'S and longitudes 70°35'W and 73°14'W (Fig. 1). The stations provide hourly rainfall measurements and are part of a national rain gauge network managed by the General Water Directorate (DGA). As shown in Table 1, the amount of data per station ranged from 3 to 28 years, adding up to a total of 418 years and 17,803 storms. Depending on the station, the rainfall data were recorded between year 1970 and 2013, with annual data missing in some stations. Missing and incomplete years were removed from the analysis to make the data used as reliable and

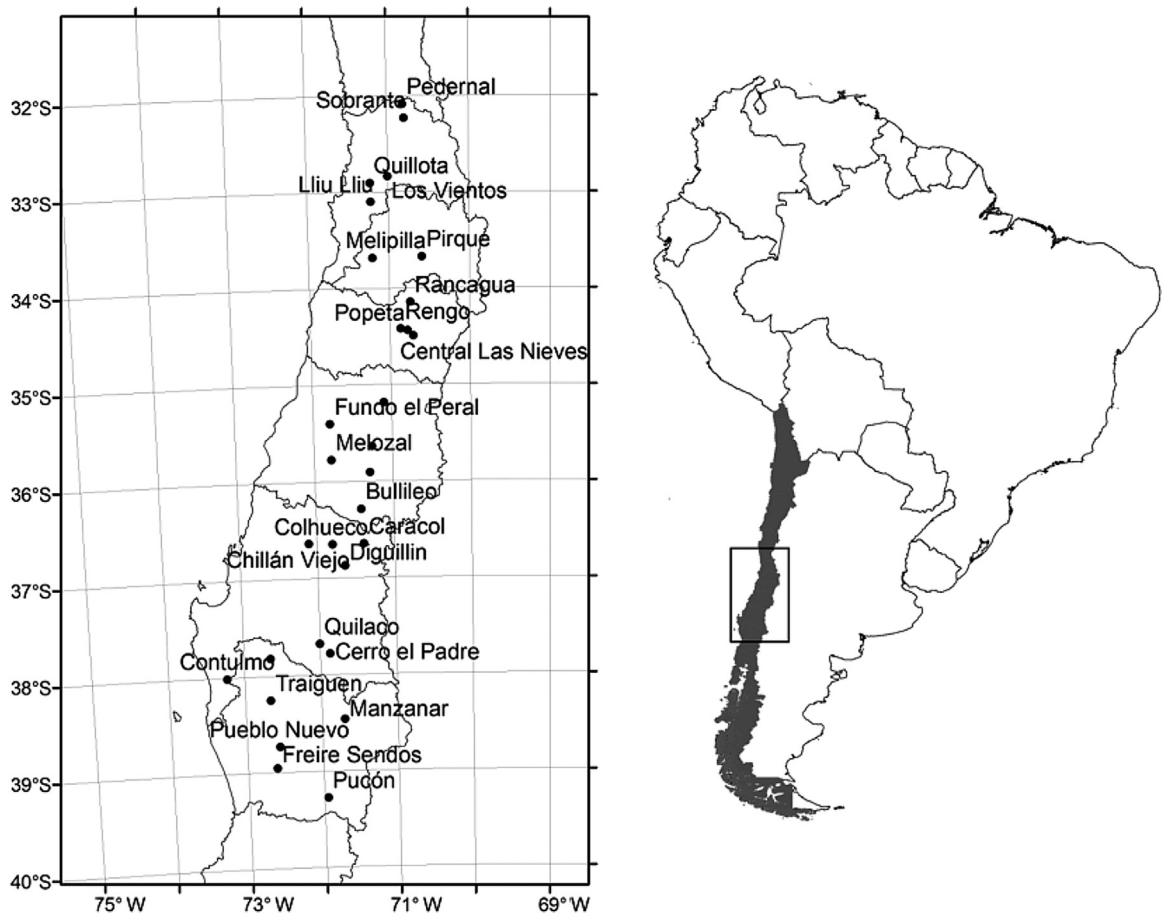

Fig. 1. Spatial distribution of the study sites.

homogenous as possible. The climate in this portion of Chile is mainly semi-arid and Mediterranean, with annual precipitations range from 35 to 1236 mm/year. Also, the rainfall in the study area is usually of a frontal nature (Escobar and Aceituno, 1998; Bonilla and Vidal, 2011), with intensities that rarely exceed 5.5 mm h^{-1} (Table 1). Additionally, the rainfall is highly erosive in some areas, and precipitation amounts increase with latitude. It must be noted that not all the records correspond to the same time period; however the quality of the data is not a limitation because this study seeks to quantify how changes in precipitation patterns alter rainfall erosivity, making these changes more important than the precipitation values observed for each station.

2.2. Estimating rainfall erosivity

The following equation was used to compute rainfall erosivity (Renard et al., 1997):

$$EI_{0.5} = \left[\sum_{k=1}^{m} 0.29[1 - 0.72exp(-0.082i_k)]\Delta V_k\right] I_{0.5} \quad (1)$$

where $EI_{0.5}$ is the rainfall erosivity of the event (MJ mm ha^{-1} h^{-1}), i_k is the rainfall intensity for the k^{th} period (mm h^{-1}), and ΔV_k is the rainfall amount (mm) for the k^{th} increment of the storm hyetograph, which is divided into m intervals and $I_{0.5}$ is the maximum 0.5-h rainfall intensity (mm h^{-1}). This equation was used because it is incorporated into the RUSLE2 model (Renard et al., 1997), making it a widely used equation for estimating rainfall erosivity, and because it provides the best fit in the study area (Lobo and Bonilla, 2015)

2.3. Climate data

2.3.1. Measured precipitation dataset

A measured rainfall dataset corresponding to hourly pluviograph records of the 28 sites described in Section 2.1 was used to develop the proposed statistical equation for estimating event-based rainfall erosivities. Using this dataset (called dataset 1), rainfall erosivity, storm duration, total precipitation, mean intensity and 0.5-h and 1-h maximum rainfall intensities were computed for every event. Because 0.5-h rainfall data are not typically recorded in Chile, these values were estimated from hourly data by fitting the following intensity-duration-frequency (IDF) curve developed by Wenzel (1982):

$$I = \frac{K}{D^n + b} \quad (2)$$

where I is the storm's mean intensity (mm h^{-1}) for duration D (h), and K, n and b are dimensionless parameters that are fitted for every storm. The intensities for durations of 1–6 h were computed and a non-linear regression technique was used to fit the data (Lobo et al., 2015). Then, the 0.5-h maximum precipitation amount was calculated for each storm, which was then used to compute $I_{0.5}$ and the rainfall erosivity of every event.

2.3.2. Simulated precipitation datasets

The statistical equation developed in this study was validated using simulated data from the stochastic weather generator CLIGEN version 5.3. CLIGEN generates daily precipitation occurrence and amount and internal storm variables, such as peak storm intensity, duration and time to peak, as well as other climate variables (Nicks et al., 1995).

Table 2
Rainfall characteristics for each precipitation dataset. Dataset 1 corresponds to the measured data, dataset 2 to the current-conditions simulated data and dataset 3 to the climate change scenarios. Here, μ and σ are the mean and standard deviations of the samples, respectively.

	Dataset 1		Dataset 2		Dataset 3	
	μ	σ	μ	σ	μ	σ
Annual rainfall (mm)	435.9	344.7	435.9	344.7	489.9	396.5
Precipitation per event (mm)	13.0	14.6	13.0	14.6	15.8	19.6
$I_{0.5}$ (mm h^{-1})	3.9	3.8	3.5	4.2	4.5	5.3
I_1 (mm h^{-1})	3.4	3.3	3.2	3.7	4.1	4.7
I_{mean} (mm h^{-1})	1.1	1.0	1.1	1.5	1.4	1.8
Storm duration (h)	14.6	16.6	14.1	5.7	11.8	5.7

Thus, this weather generator provides instant rainfall intensities for every simulated storm, which allows computing $I_{0.5}$ and rainfall erosivity without any assumption or IDF curve. CLIGEN generates rainfall events of up to 24 h; however, when an event of 24 h was immediately followed by another event, it was assumed that both correspond to the same rainfall event when computing erosivity. Two datasets were simulated using CLIGEN, one with the current rainfall conditions of Central Chile, and another with changes in precipitation amounts and/or rainfall intensities. The first simulated dataset (called dataset 2) was constructed by implementing CLIGEN with measured daily precipitation data and the procedures described in the study of Lobo et al. (2015). This dataset was meant to reflect the current conditions of precipitation in Central Chile. The second simulated dataset corresponds to a series of modifications of the simulated current conditions dataset, where rainfall intensities and amounts were modified (called dataset 3). Adjustments were made to the input data and CLIGEN files so that the weather generator provided data with changes in rainfall intensities alone, precipitation alone and both variables. These changes were meant to reflect potential climate change scenarios where precipitation amounts per event and/or intensities tend to increase, but the specific augments were randomly chosen. This was done to prove that the developed equation holds for any change in the rainfall patterns and not those described by a specific model. Table 2 shows a summary of the main rainfall characteristics of the 3 datasets.

2.4. Statistical analysis

To develop the statistical equation for estimating the event-based rainfall erosivity, several variables, including storm duration, total precipitation, mean intensity and 0.5-h and 1-h maximum rainfall intensities, were related to erosivity. These variables were chosen as they are commonly used to describe rainfall patterns (Wischmeier and Smith, 1978) and were extracted from the measured dataset described in the measured precipitation dataset section (dataset 1). All the extracted variables and their combinations were correlated to erosivity, which allowed identifying the main variables controlling it. A regression curve between the variables showing the highest correlation with rainfall erosivity was then fitted, and the obtained relationship was tested with the simulated precipitation datasets (dataset 2 and 3). This allowed evaluating the robustness of the developed relationship to changes in precipitation patterns, which is necessary to assess its predictive power under different climate change scenarios.

It should be noted that the meteorological stations used to calibrate the statistical equation have different number of recorded rainfall events, meaning that some stations had a larger impact on the regression constants than others. However, the stations with large number of events are scattered throughout the entire study area, reducing the bias that results from the overrepresentation of certain stations. Nevertheless, this is a limitation of the proposed equation that should be considered in its interpretation.

Table 3
Coefficient of determination R^2 between different rainfall properties and rainfall erosivity for the measured rainfall data. The variables are the event's precipitation (P), duration (D), mean intensity (I_{mean}) and maximum 0.5 and 1-h rainfall intensity ($I_{0.5}$ and I_1, respectively).

	R^2
P (mm)	0.54
D (h)	0.00
I_{mean} (mm h^{-1})	0.55
I_1 (mm h^{-1})	0.73
$I_{0.5}$ (mm h^{-1})	0.75

Table 4
Coefficient of determination R^2 between the product of different rainfall properties and rainfall erosivity for the measured rainfall data (for example, the product of P and D has a R^2 with erosivity of 0.36). The variables are the event's precipitation (P), duration (D), mean intensity (I_{mean}) and maximum 0.5 and 1-h rainfall intensity ($I_{0.5}$ and I_1, respectively).

	D (h)	I_{mean} (mm h^{-1})	I_1 (mm h^{-1})	$I_{0.5}$ (mm h^{-1})
P (mm)	0.36	0.79	0.92	0.97
D (h)		0.54	0.53	0.54
I_{mean} (mm h^{-1})			0.61	0.61
I_1 (mm h^{-1})				0.83
$I_{0.5}$ (mm h^{-1})				0.75

3. Results and discussion

3.1. Proposed rainfall erosivity equation

Table 3 shows the R^2 values between rainfall erosivity and different rainfall variables. As shown, each variable by itself does not explain more than 75% of the variability of rainfall erosivity, where the highest R^2 value is observed for the maximum 0.5-h rainfall intensity $I_{0.5}$ (R^2 = 0.75). Storm duration, D, shows no relation with rainfall erosivity (R^2 = 0), which is likely because of the frontal nature of the rainfall in Chile, where storm duration is not generally related to rainfall intensity, unlike convective systems (Escobar and Aceituno, 1998). Because erosivity is dominated by rainfall intensity, this result was expected; however, it is probably not the case for convective storms. As shown in Table 4, when multiplying the variables among each other, high R^2 values are observed, especially when combining total precipitation amounts with $I_{0.5}$, where the product $P{\cdot}I_{0.5}$ explains almost all the variability of rainfall erosivity (R^2 = 0.97). High R^2 values are also observed for the product of P and the other rainfall intensities, I_1 and I_{mean}, showing that the product of P and a measure of maximum rainfall intensity are enough to predict rainfall erosivity at the event level. No other combinations of variables were tested because of the high R^2 values obtained with the product of P and rainfall intensity.

The strong relationship found between erosivity and $P{\cdot}I_{0.5}$ is explained by Eq. (1), in which erosivity is the product of the rainfall kinetic energy E and $I_{0.5}$. E is a function of the storm hyetograph and therefore depends on the different rainfall intensities throughout the storm (Rosewell, 1986; van Dijk et al., 2002; Salles et al., 2002; Lobo and Bonilla, 2015). However, as shown in Fig. 2, E correlates highly with P, showing that the shape of the hyetograph is irrelevant when estimating erosivity in the study area. Therefore, the product of $I_{0.5}$ and P can be used to accurately estimate rainfall erosivity in the study area rather than the product of $I_{0.5}$ and E.

Fig. 3 compares the rainfall erosivity to $P{\cdot}I_{0.5}$, where a strong correlation between the variables is evident. The variables were related

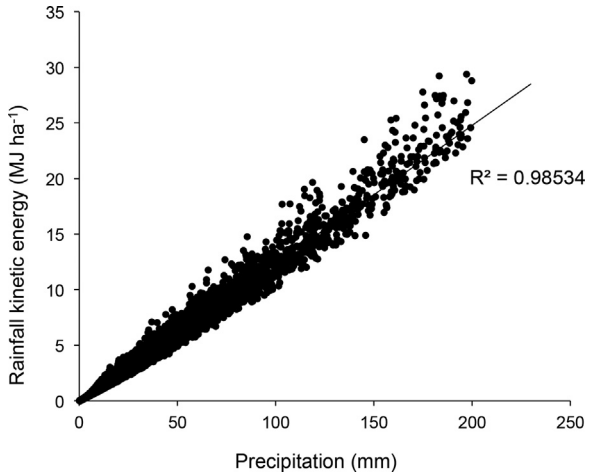

Fig. 2. Relationship between precipitation per event and rainfall kinetic energy. As shown, a strong relationship was found between the variables (R^2 = 0.98).

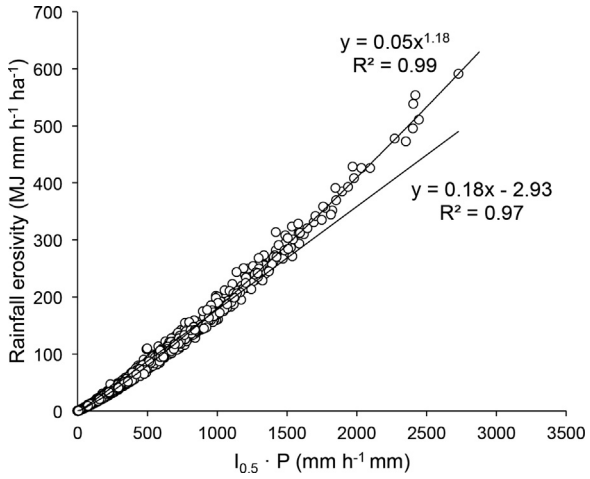

Fig. 3. Relationship between the product of the rainfall event's maximum 0.5-h rainfall intensity ($I_{0.5}$) and total precipitation (P) with rainfall erosivity. The relationship between the variables is best described as nonlinear, as the linear regression is not effective for erosivity values over 300 MJ mm h^{-1} ha^{-1} per event.

using the following equation:

$$EI_{0.5} = a(P \bullet I_{0.5})^b \quad (3)$$

where a and b are dimensionless parameters with values of 0.051 and 1.184, respectively, for dataset 1. This equation was used because a nonlinear relationship provided a better fit between erosivity and $P{\cdot}I_{0.5}$, with a R^2 of 0.99, compared to 0.97 of that of a linear regression (Fig. 3). The value of a may be interpreted as the average kinetic energy provided by a rainfall event of magnitude P, while b accounts for deviations from linearity. This nonlinear relationship allows for accurate estimations of high erosivity values, which is not the case with the linear regression, as shown in Fig. 3.

To test the predictive power of the calibrated Eq. (3) under different potential climate change scenarios, the simulated datasets were used to test whether Eq. (3) provided accurate erosivity estimates. Eq. (3) was first tested with the CLIGEN simulated data for the current conditions (dataset 2). This was done to test whether the equation is robust enough to predict changes in rainfall patterns, as CLIGEN simulates storms that are very different to those existing in Central Chile (Lobo et al., 2015). CLIGEN simulates storms with convective patterns, where intensities increase exponentially to a peak value and then decrease in the same way (Nicks et al., 1995). On the other hand, the rainfall intensities of the frontal storms in Central Chile are usually constant, where the peak intensity is not very different to the mean rainfall intensity (Escobar and Aceituno, 1998). As shown in Fig. 4, Eq. (3) provided accurate erosivity values for the CLIGEN-simulated storms, regardless of this difference in storm patterns. The Nash-Sutcliffe efficiency (N-S) of Eq. (3) for the CLIGEN simulations is identical to that of the measured data (N-S = 0.99), showing that the developed relationship is robust when changing rainfall patterns are observed. This demonstrates that Eq. (3) can be used to compute rainfall erosivity in changing rainfall patterns due to climate change in the study area.

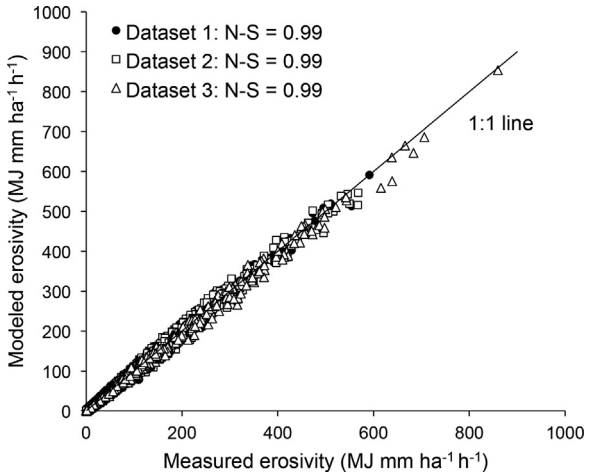

Fig. 4. Comparison between the measured and modeled erosivity values when using Eq. (3) for the measured data (dataset 1), the current-conditions simulated data (dataset 2) and the climate change scenarios (dataset 3). Even if the equation was calibrated using dataset 1, it proved to provide accurate estimates for datasets 2 and 3.

Eq. (3) was also tested for changes in rainfall intensities and amounts by implementing it with dataset 3, in which different climate change scenarios were simulated (Table 2). As shown in Fig. 4, the equation provides the same fit as for the measured data (dataset 1) and dataset 2, with an N-S efficiency of 0.99. This shows that Eq. (3) is robust for changes in precipitation amounts and intensities in the study sites and can be used for effectively estimating rainfall erosivity at the storm level in the study area. Moreover, the performance of the equation in every simulation shows that it is not necessary to predict rainfall patterns at all when estimating erosivity at the storm level. Only accurate estimations of rainfall precipitation and maximum 0.5-h rainfall intensities are needed, which simplifies the number of variables required when estimating rainfall erosivity in climate change scenarios.

3.2. Expanding the proposed equation to other measures of maximum rainfall intensity

Despite the strong relationship found between $P{\cdot}I_{0.5}$ and rainfall erosivity, its usefulness for predicting erosivity under climate change scenarios is limited by the time resolution of the precipitation forecasts of GCMs. Currently, most long-term forecasts are downscaled to provide daily precipitation estimates, where $I_{0.5}$ cannot be obtained for implementing Eq. (3) (Minville et al., 2008; Nearing et al., 2005; Yang et al., 2003). Short-term forecasts usually have a higher time resolution, where precipitation is estimated in fixed time intervals, such as every 3, 1 or 0.5 h. However, these time intervals are not always suitable for estimating $I_{0.5}$, which also limits the applicability of Eq. (3). Therefore, Eq. (3) was redefined to estimate rainfall erosivity at different resolutions of precipitation data, where erosivity was estimated as follows:

$$EI_{0.5} = a(P \bullet I_X)^b \quad (4)$$

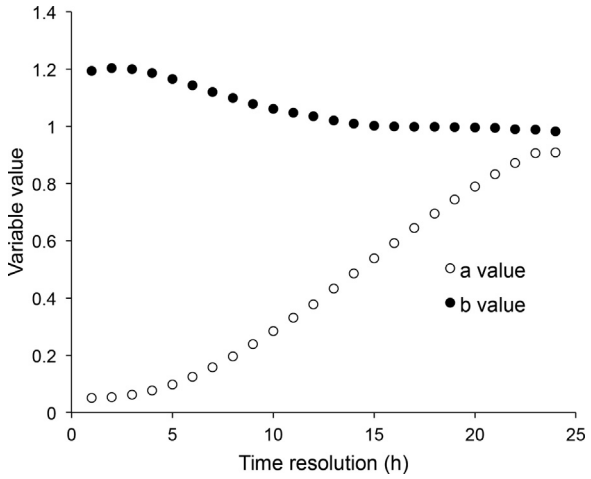

Fig. 5. Values of the constants a and b used in Eq. (4) for estimating rainfall erosivity with rainfall data at different time resolutions. Each of the 24 points per variable represents the value of the variables for a specific time resolution between 1 and 24 h, with one point per hour. The values of a and b were calibrated using the measured data (dataset 1).

where I_X is the maximum rainfall intensity for rainfall data with a time resolution of X h. This was done because, as shown in Table 4, the product of the total rainfall and the mean rainfall intensity are correlated to erosivity in the study site ($R^2 = 0.79$). Just like Eqs. (3) and (4) was calibrated using the measured dataset (dataset 1) and then tested for simulated datasets 2 and 3. However, 24 different calibrations were performed, one for each hour between time resolutions of 1 h and 24 h. This was done by aggregating the hourly data and obtaining the values of I_X for each time resolution. The values of the regression constants a and b are shown in Fig. 5 for the various time resolutions, which were used with Eq. (4) for computing the erosivity for the CLIGEN-simulation datasets.

Fig. 6 shows the performance of Eq. (4) for time resolutions of 1 through 24-h for all datasets 1, 2 and 3, while Table 5 shows its performance for the 1-h and 24-h time resolutions ($I_{0.5}$ event and I_{24} event, respectively). As shown in the figure, the equation provides consistent results in every dataset, showing almost no difference among them for every time resolution. This demonstrates the robustness of the equation in the study area, as it was calibrated using dataset 1 and provided consistent results for datasets 2 and 3. Additionally, as shown in the figure, Eq. (4) provides accurate erosivity estimates for a 1-h time resolution (N-S = 0.99 for every dataset), with decreasing efficiencies as the time resolution decreases. The lowest N-S efficiency value is observed for the 24-h time resolution in dataset 3, with an N-S efficiency of 0.75 (Table 5), proving that Eq. (4) may be used to predict erosivity for every time resolution between 1 and 24 h. Therefore, Eq. (4) is a robust alternative for computing rainfall erosivity when changes in precipitation patterns and amounts are observed, as it indirectly establishes a conversion factor between I_X and $I_{0.5}$, which is reflected in the variables a and b. Moreover, because a 24-h time resolution can be computed directly from daily rainfall, Eq. (4) may be used to predict daily rainfall erosivity with data available from most GCM forecast downscaling methods. However, if these methods were to provide higher resolution data, better erosivity predictions could be obtained, as shown in Fig. 6. This equation is thus a simple alternative to other statistical downscaling methods, such as the one described by Panagos et al. (2017), as it provides accurate estimates using only measured precipitation pattern information.

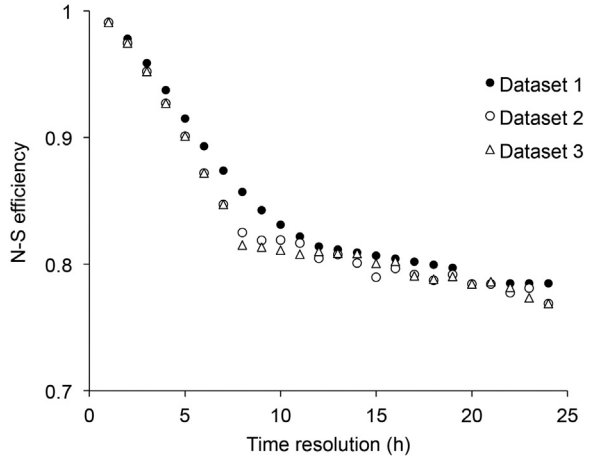

Fig. 6. Nash-Sutcliffe (N-S) efficiency between the measured and modeled rainfall erosivity per event when using Eq. (4) with data at different time resolutions. The N-S efficiency values are shown for the measured data (dataset 1), the current-conditions simulated data (dataset 2) and the climate change scenarios (dataset 3). Even if the equation was calibrated using dataset 1 for each time resolution, it provided accurate estimates for datasets 2 and 3.

Table 5
Performance of the event and annual-based equations for estimating rainfall erosivity, where n is the number of events (or years in the case of the annual data), and N-S is the Nash Sutcliffe efficiency between the measured and modeled erosivity values.

		n	N-S	R^2	Slope
Dataset 1	$I_{0.5}$ event	17803	0.99	0.97	1.00
	I_{24} event	17803	0.78	0.79	1.03
	$I_{0.5}$ annual	404	0.99	0.99	1.00
	I_{24} annual	404	0.92	0.93	1.03
	Modified Fournier index	404	− 1.29	0.00	0.00
	Precipitation index	404	0.84	0.84	0.97
Dataset 2	$I_{0.5}$ event	17803	0.99	0.97	1.00
	I_{24} event	17803	0.78	0.79	1.03
	$I_{0.5}$ annual	404	0.99	0.99	1.00
	I_{24} annual	404	0.85	0.87	0.89
	Modified Fournier index	404	0.01	0.00	0.00
	Precipitation index	404	0.70	0.75	0.80
Dataset 3	$I_{0.5}$ event	17803	0.99	0.99	1.01
	I_{24} event	17803	0.75	0.77	1.14
	$I_{0.5}$ annual	404	0.99	0.99	0.99
	I_{24} annual	404	0.89	0.91	0.92
	Modified Fournier index	404	− 1.24	0.00	0.00
	Precipitation index	404	0.72	0.81	0.78

The good performance of Eq. (4) demonstrates that a measure of maximum rainfall intensity and total precipitation are enough to predict daily rainfall erosivity when changes in precipitation patterns and/or amounts are observed. This finding is of importance when downscaling the output of GCMs into soil loss models, as it provides two critical variables that need to be carefully considered when using current downscaling techniques. When climate simulators are used for this purpose, the user must consider whether to modify the rainfall patterns, the precipitation amounts or both, because, as demonstrated in Eq. (4), both affect erosivity in different measures. Rainfall patterns affect I_X, while precipitation amounts control P, so deciding which to modify will affect erosivity in different ways. Therefore, when using climate generators to downscale daily GCM forecasts, a sensibility analysis should be performed for the variables controlling precipitation patterns and amounts, as monthly or daily forecasts alone do not provide information on the rainfall patterns, which affect I_X. This is particularly important for the method described by Nearing et al. (2004), in which CLIGEN is used to downscale GCM forecasts.

On the other hand, when using empirical methods to convert GCM forecasts into daily or annual rainfall erosivity values, care should be taken when choosing the appropriate empirical equation. Most empirical relationships, such as those using the modified Fournier index (Arnoldus, 1980) have not been tested under potential climate change

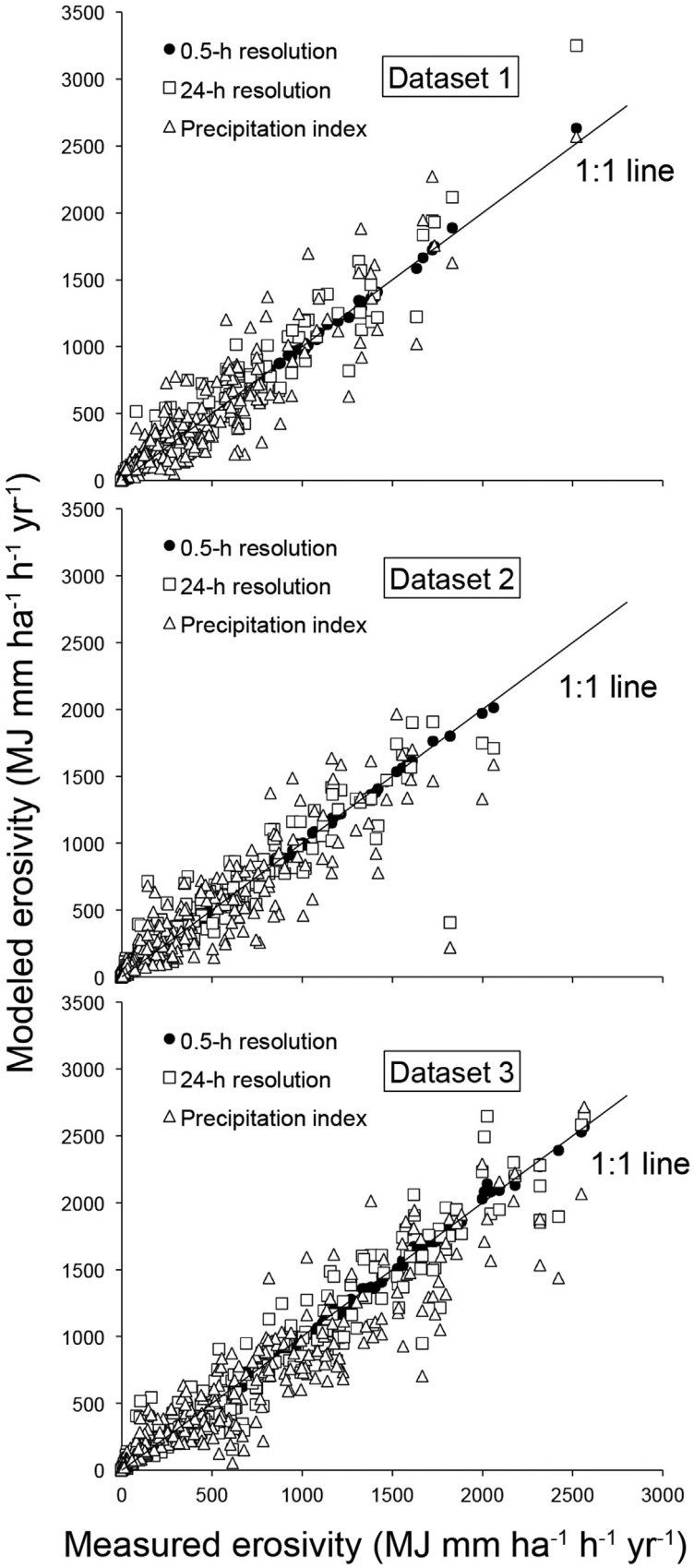

Fig. 7. Comparison between the measured and modeled annual erosivity estimates when using Eq. (4) for the 0.5 and 1-h time resolutions and the precipitation index (Eq. (5)) for datasets 1, 2 and 3. As shown Eq. (4), with a time resolution of 0.5-h, provides highly accurate results regardless of dataset. Eq. (4) with the 24-h time resolution and Eq. (5) provide similar results for datasets 1 and 2. However, for dataset 3, the dispersion of Eq. (5) increases, showing that it is not a robust equation when precipitation amounts and intensities change.

scenarios and could provide inaccurate erosivity values when GCM forecasts are used. Therefore, when using such relationships to assess soil loss under climate change scenarios, a prior study should be performed to verify whether those equations hold when changes in precipitation and/or rainfall patterns are observed. Simulations such as the ones performed in this study provide an alternative way to validate these equations.

3.3. Estimating annual rainfall erosivity using the proposed equation

Thus far, Eq. (4) has been used to provide daily erosivity estimates, which are useful when using empirical soil loss models working at a daily scale, such as the RUSLE2. However, the most widely used soil loss model is the RUSLE (Kinnell, 2010), which uses annual erosivity values. Therefore, annual erosivity values were computed by adding the daily outputs of Eq. (4) to assess whether the proposed equation yields accurate annual soil loss estimates. These estimates were compared against the measured annual erosivity values obtained using the yearly summations of Eq. (1) for every rainfall event. Moreover, the performance of two commonly used relationships, the modified Fournier Index and the annual precipitation index (Renard et al., 1991), were also evaluated. The models used are the following:

$$R = a \cdot P_{annual}^{b} \quad (5)$$

$$R = c \cdot F^{d} \quad (6)$$

$$F = \frac{\sum_{r=1}^{12} P_r^2}{P_{annual}} \quad (7)$$

Where R is the annual rainfall erosivity (MJ mm ha^{-1} h^{-1} yr^{-1}), P_{annual} is the annual precipitation amount (mm); F is the modified Fournier Index; P_r is the total precipitation for month r (mm); and a, b, c and d are regression constants. Eqs. (5) and (6) were calibrated using the measured dataset and then tested for the simulated data.

Fig. 7 shows the performance of Eq. (4) for the 1 and 24-h time resolution data when estimating annual erosivity, as well as the performance of Eq. (5) for the measured and simulated datasets. The performance of Eq. (6) was not shown because the modified Fournier index showed no correlation with annual erosivity in the study area (Table 5). As shown, Eq. (4) provides highly accurate annual erosivity estimates, even at a 24-h time resolution, regardless of the dataset used. The lowest observed N-S efficiency is 0.85 for dataset 2 (Table 5), demonstrating the robustness of the equation for computing both daily and annual erosivity for current climates and potential climate change scenarios. In the case of the empirical relationship using the annual precipitation index, Eq. (5), a good performance was observed for dataset 1, as shown in Tables 5 (N-S = 0.84). However, for datasets 2 and 3, the model's performance decreased, with an N-S efficiency of 0.70 and 0.72, respectively. This shows that the total annual precipitation is a good index for estimating annual rainfall erosivity when total precipitation and intensities do not change drastically. However, when changes are observed in precipitation patterns and amounts, the equation is not as robust as Eq. (4). On the other hand, the modified Fournier index did not show any correlation with annual erosivity regardless of the dataset (Table 5). This is likely because the Fournier index assumes that months with high rainfall will have a higher impact on rainfall erosivity, as large rainfalls are usually associated with higher rainfall intensities (Arnoldus, 1980). However, this is not the case of the frontal storms observed in the study area, where rainfall intensity is not related to storm duration.

3.4. Model limitations

Like any other empirical relationship, Eq. (4) has limitations that should be considered when using it to estimate daily and annual erosivity. First, the relationship was tested only in the study area; therefore, its effectiveness was demonstrated only for Central Chile. However, because of the large rainfall gradient existing from north to south in the study area (Table 1), Eq. (4) can be applied in a wide variety of conditions, suggesting that it may be extrapolated to locations with a similar climate. Moreover, the equation provided robust results in every simulation dataset, which included storms that are not typical of the frontal systems existing in Central Chile (Table 2). This shows that Eq. (4) could be applied to storms other than those of a frontal nature. However, its performance in other types of storms should be tested firsthand to verify its effectiveness, particularly under convective storm patterns.

Another limitation of Eq. (4) is that its capability for predicting the erosivity of potential climate change scenarios was only tested for CLIGEN simulations, providing accurate results for storms with the rainfall patterns described by Nicks et al. (1995). Other climate generators may use different rainfall patterns, which might affect the performance of the proposed equation. However, because the equation was always calibrated using the measured storm data and then tested with the CLIGEN simulations, its applicability was demonstrated for two completely different types of storms. This shows that the effectiveness of the equation does not completely depend on the rainfall patterns, but rather on the maximum rainfall intensity and total precipitation. Therefore, Eq. (4) should provide effective results when using other climate simulators.

Even though Eq. (4) has limitations, its simplicity and good performance in the study area demonstrate that it is an alternative for effectively predicting rainfall erosivity under different climate change scenarios. The equation depends exclusively on the total precipitation and a measure of maximum rainfall intensity, where better results are obtained when rainfall data with higher time resolutions are used. Currently, most GCM downscaling methods do not usually provide detailed storm forecasts and therefore maximum rainfall intensities other than I_{24} cannot be obtained to use Eq. (4). The equation provided good erosivity estimates when using I_{24}, making it applicable with daily precipitation data from current GCM downscaling methods. However, its accuracy increases dramatically when finer rainfall intensity data are used, which highlights the need of higher resolution data or novel downscaling methods for estimating the maximum rainfall intensity. This study demonstrates that if, for instance, $I_{0.5}$ is obtained from GCM forecasts, erosivity could be predicted with nearly 99% accuracy. Therefore, for modeling soil loss under climate change scenarios, efforts should be made for accurately estimating the maximum rainfall intensity rather than the whole distribution of the rainfall. In addition, Eq. (4) provides a tool that can be readily used with daily precipitation from current GCM downscaling methods for accurately estimating rainfall erosivity, but its limitations should always be considered.

4. Conclusions

A simple statistical equation for accurately estimating the rainfall erosivity of individual storms under changing precipitation patterns was developed. This equation uses the product of each storm's total precipitation and a measure of its maximum rainfall intensity, which are parameters that may be easily obtained from downscaled GCM data to predict changes in rainfall erosivity. The equation was calibrated using measured precipitation data from 28 sites in Central Chile and then tested with simulated data from the CLIGEN weather generator, which was meant to simulate potential climate change scenarios in the study area.

This study demonstrates that the equation provides accurate erosivity estimates in the study area, where better results were obtained when the maximum rainfall intensity used approached the maximum 0.5-h rainfall intensity, $I_{0.5}$. The equation provided erosivity estimates with a R^2 ranging from 0.78 to 0.99; the lowest value was obtained when using I_{24}, while the highest when using $I_{0.5}$. This shows that obtaining a measure of the maximum rainfall intensity with climate

change forecast tools is paramount when estimating rainfall erosivity and soil loss in climate change scenarios.

The developed equation was calibrated and validated for Central Chile; however, because of the different rainfall patterns analyzed, and the large precipitation gradients that exist from north to south, the methodology used in this study may be applied to a wide variety of conditions. Nevertheless, its effectiveness was not demonstrated for other locations, particularly those with highly different rainfall patterns. Thus, the methodology needs to be tested further for applying it at a larger scale. If successful, the methodology could be used to compute regression factors for several regions worldwide, making it easy to compute rainfall erosivity from downscaled GCM data.

The equation developed in this study is meant to be used as a simple tool for predicting rainfall erosivity under climate change scenarios, particularly in locations where climate data is scarce. However, it also allowed the identification of critical variables for predicting erosivity, highlighting the importance of obtaining a measure of maximum rainfall intensity in GCM forecasts or downscaling methods rather than the complete distribution of the rainfall. Models such as this one allows the incorporation of GCM forecasts into simple soil loss models that use daily rainfall erosivity so that better and more sustainable soil and water conservation practices can be developed.

Acknowledgments

This research was supported by funding from the National Commission for Scientific and Technological Research, Chile, Grant CONICYT/FONDECYT/Regular 1161045. The rainfall data were provided by the General Directorate of Water Resources (DGA), Government of Chile.

References

Arnoldus, H.M.J., 1980. An approximation of the rainfall factor in the Universal Soil Loss Equation. In: Boodt, M. De, Gabriels, D. (Eds.), Assessment of Erosion. Wiley, Chichester, UK, pp. 127–132.

Asselman, N.E.M., Middelkoop, H., van Dijk, P.M., 2003. The impact of changes in climate and land use on soil erosion, transport and deposition of suspended sediment in the River Rhine. Hydrol. Process. 17, 3225–3244.

Boardman, J., Favis-Mortlock, D.T., 1993. Climate change and soil erosion in Britain. Geogr. J. 159 (2), 179–183.

Bonilla, C.A., Vidal, K.L., 2011. Rainfall erosivity in Central Chile. J. Hydrol. 410 (1–2), 126–133.

Burton, A., Fowler, H.J., Blenkinsop, S., Kilsby, C.G., 2009. Downscaling transient climate change using a Neyman – Scott rectangular pulses stochastic rainfall model. J. Hydrol. 381, 18–32.

Erol, A., Randhir, T.O., 2013. Watershed ecosystem modeling of land-use impacts on water quality. Ecol. Model. 270, 54–63. https://doi.org/10.1016/j.ecolmodel.2013.09.005.

Escobar, F., Aceituno, P., 1998. Influencia del fenómeno ENSO sobre la precipitación nival en el sector andino de Chile central durante el invierno. Bull. De. l'Institut Fr. Détudes Andin. 27 (3), 753–759.

Foster, G.R., 2008. Revised Universal Soil Loss Equation Version 2 (RUSLE2). (U.-A. R. Service, Ed.) (Vol. 2). Washington DC.

Hoomehr, S., Schwartz, J.S., Yoder, D.C., 2016. Potential changes in rainfall erosivity under GCM climate change scenarios for the southern Appalachian region, USA. Catena 136, 141–151.

Kinnell, P.I.A., 2010. Event soil loss, runoff and the Universal soil loss equation family of models: a review. J. Hydrol. 385, 394–397.

Klik, A., Eitzinger, J., 2010. Impact of climate change on soil erosion and the efficiency of soil conservation practices in Austria. J. Agric. Sci. 148, 529–541.

Lobo, G.P., Bonilla, C.A., 2015. Sensitivity analysis of kinetic energy-intensity relationships and maximum rainfall intensities on rainfall erosivity using a long-term precipitation dataset. J. Hydrol. 527, 788–793.

Lobo, G.P., Frankenberger, J.R., Flanagan, D.C., Bonilla, C.A., 2015. Evaluation and improvement of the CLIGEN model for storm and rainfall erosivity generation in Central Chile. Catena 127, 206–213.

Minville, M., Brissette, F., Leconte, R., 2008. Uncertainty of the impact of climate change on the hydrology of a nordic watershed. J. Hydrol. 358, 70–83.

Mondal, A., Khare, D., Kundu, S., 2016. Change in rainfall erosivity in the past and future due to climate change in the central part of India. Int. Soil Water Conserv. Res. 4 (3), 186–194.

Morrison, J., Quick, M.C., Foreman, M.G.G., 2002. Climate change in the Fraser River watershed: flow and temperature projections. J. Hydrol. 263, 230–244.

Nearing, M.A., 2001. Potential changes in rainfall erosivity in the U.S. with climate change during the 21st century. J. Soil Water Conserv. 56 (3), 229–232.

Nearing, M.A., Garbrecht, J.D., Steiner, J.L., 2004. Downscaling monthly forecasts to simulate impacts of climate change on soil erosion. Soil Sci. Soc. Am. J. 68, 1376–1385.

Nearing, M.A., Jetten, V., Baffaut, C., Cerdan, O., Couturier, A., Hernandez, M., van Oost, K., 2005. Modeling response of soil erosion and runoff to changes in precipitation and cover. Catena 61 (2–3), 131–154.

Nicks, A.D., Lane, L.J., Gander, G.A., 1995. Weather generator. In: Flanagan, D.C., Nearing, M.A. (Eds.), Water Erosion Prediction Project: Hillslope Progile and Watershed Model Documentation. USDA-ARS National Soil Erosion Research Laboratory, West Lafayette, pp. 1–22.

Panagos, P., Ballabio, C., Meusburger, K., Spinoni, J., Alewell, C., Borrelli, P., 2017. Towards estimates of future rainfall erosivity in Europe based on REDES and WorldClim datasets. J. Hydrol. 548, 251–262.

Renard, K.G., Foster, G.R., Weesies, G.A., Porter, J.P., 1991. RUSLE Revised universal soil loss equation. J. Soil Water Conserv. 46 (1).

Renard, K.G., Foster, G.R., Weesies, G.A., McCool, D.K., Yoder, D.C., 1997. Predicting soil erosion by water: a guide to conservation planning with the Revised Universal Soil Loss Equation (RUSLE). USDA Agricultural Handbook No 703. Washington DC, USDA.

Rosewell, C.J., 1986. Rainfall kinetic energy in Eastern Australia. J. Clim. Appl. Meteorol. 25, 1695–1701.

Salles, C., Poesen, J., Sempere-Torres, D., 2002. Kinetic energy of rain and its functional relationship with intensity. J. Hydrol. 257, 256–270.

Samadi, S.Z., Sagareswar, G., Tajiki, M., 2010. Comparison of General Circulation Models: methodology for selecting the best GCM in Kermanshah Synoptic Station, Iran Gummeneni Sagareswar. Int. J. Glob. Warm. 2 (4), 347–365.

van Dijk, A.I.J., Bruijnzeel, L.A., Rosewell, C.J., 2002. Rainfall intensity - kinetic energy relationships: a critical literature appraisal. J. Hydrol. 261, 1–23.

von Storch, H., 1999. On the use of "'Inflation'" in statistical downscaling. Am. Meteorol. Soc. 12, 3505–3506.

Wenzel, H., 1982. Rainfall for urban stormwater design, 7th ed. Urban Storm Water Hydrology 7 American Geophysical Union, Washington DC.

Wischmeier, W.H., Smith, D.D., 1978. Predicting rainfall erosion. Agriculture Handbook No. 537. United States Department ofAgriculture, Washington D.C.

Xu, C., 1999. From GCMs to river flow: a review of downscaling methods and hydrologic modelling approaches. Progress. Phys. Geogr. 23 (2), 229–249.

Yang, D., Kanae, S., Oki, T., Koike, T., Musiake, K., 2003. Global potential soil erosion with reference to land use and climate changes. Hydrol. Process. 17, 2913–2928.

Yu, B., 2005. Adjustment of CLIGEN parameters to generate precipitation change scenarios in southeastern Australia. Catena 61, 196–209.